RSC Advances

PAPER

View Article Online
View Journal | View Issue

Cite this: *RSC Adv.*, 2023, **13**, 7656

Chemotherapeutic-caused liver toxicity hinders nanomedicine development‡

Pengfei Wu,† Yuhang Zhang,† Shiyao Zhu,† Mo Wang, Peng Zhou, Guishuan Wang* and Wenqing Li *

Received 21st December 2022
Accepted 21st February 2023

DOI: 10.1039/d2ra08148b

rsc.li/rsc-advances

Few nanomedicines are approved for clinical cancer treatment as only about 0.7% (median) of nanoparticles enter solid tumors. Nanomedicine as the second medication is usually used in cancer treatment after chemotherapy, immunotherapy surgery, or radiotherapy treatment. However, it is currently unpredictable whether the priority treatment enhances or reduces the therapeutic effect of nanomedicine. Here, by considering prior chemotherapy (5-FU or cisplatin treatment), immunotherapy (IL-2, IL-6, or IL-21-treatment), or phosphate-buffered saline (PBS treatment), we compared the biodistribution of AuNPs in the liver, spleen, kidney, and tumor. We found that the accumulation of AuNPs in the liver and spleen increased in cisplatin pretreatment compared to the PBS treatment, while there was no significant effect on the accumulation of AuNPs in the tumor due to cisplatin-induced significant liver damage while other treatments did not change the biodistribution of AuNPs in the liver, spleen, kidney, and tumor. These results indicated that cisplatin pretreatment is not suitable for subsequent nanomedical cancer therapy. Our work opens a new insight to design low-toxicity chemotherapy to be applied before nanomedicine.

Introduction

Engineering nanoparticles for delivering chemotherapy drugs can improve therapeutic efficacy over conventional chemotherapy in cancer treatment but few nanoparticles have been approved for clinical applications.[1–4] One reason is that too few nanoparticles enter solid tumors. A meta-analysis data showed that about 0.7% (median) of nanoparticles were successfully delivered into solid tumors, which may be because of the mononuclear phagocytic system, where a combination of cellular and physical properties lead to the sequestering of most of the nanoparticles.[5,6] Previous studies showed that when nanoparticles entered the liver, the flow rate of the nanoparticles slowed 1000 times in the liver sinusoid. Most of the nanoparticles were taken up by hepatic Kupffer cells, B cells, and endothelial cells.[7] Manipulating the size, shape, or surface modification of nanoparticles is the most common method to prevent phagocytic uptake by the liver, but this still has finite potential to solve the phagocytic uptake for promoting nanomedicine therapy in clinical uses. Therefore, nanoparticle treatments are usually used as second medication in cancer treatment after chemotherapy, immunotherapy, surgery, or radiotherapy treatment.

Chemotherapy and immunotherapy are the priority treatments for cancer patients.[8–10] Chemical drugs usually lead to different liver toxicities, causing toxicity of hepatic Kupffer cells, B cells, endothelial cells, and hepatocytes. Cisplatin is the first FDA-approved metal-based anticancer drug, the mechanisms of which include the generation of DNA lesions by interacting with purine bases on DNA, forming reactive oxygen species (ROS), and activating several signal transduction pathways to cause cell apoptosis. However, cisplatin induces side effects in the body, such as hepatotoxicity, nephrotoxicity, gastrointestinal toxicities, and renal toxicity.[11,12] Besides, 5-fluorouracil (5-FU) is also widely used in cancer treatment. 5-FU can catabolize dihydropyrimidine dehydrogenase to dihydrofluorouracil in the liver, which inhibits thymidylate synthase and the incorporation of its metabolites into RNA and DNA. 5-FU also shows side effects on immune inhibition and liver damage.[13–15] Cytokines and cytokine receptors have been extensively investigated as immunotherapy for cancer patients.[16] Enhancing the growth inhibitory and immunostimulatory effects of interferons and interleukins (IL-2, IL-21, IL-7, IL-12, and IL-15), as well as inhibiting the inflammatory and tumor-promoting actions of cytokines (IL-6, TNF, and IL-1β) are common preclinical therapeutic strategies. Cytokine-based therapies show potential immune-related toxicities.[16–20]

Currently, nanoparticle treatments are used as the second medication in cancer treatment after chemotherapy and

Institute of Reproductive Medicine, School of Medicine, Nantong University, Nantong, 226000, China. E-mail: gswang@ntu.edu.cn; liwenqing505@ntu.edu.cn

‡ Electronic supplementary information (ESI) available. See DOI: https://doi.org/10.1039/d2ra08148b

† These authors contributed equally to this work

immunotherapy. Nanomedicine is usually utilized with cancer patients with a damaged liver due to the toxicity of chemotherapy or immunotherapy. The liver is the largest organ and central organ for taking up nanoparticles. Investigating the relationship between nanoparticles and the liver would be beneficial for tumor treatment. Therefore, there are two thorny questions: (I) is there a difference in the nanoparticle uptake between the normal liver and damaged liver? (II) Does the damaged liver impact nanoparticles entering to the solid tumor?

To address these questions, we pretreated tumor-bearing mice with an acute chemotherapy treatment (5-FU or cisplatin-treated mice) or immunotherapy (IL-2, IL-6, or IL-21-treated mice), which may cause damaged liver. Then, we injected gold nanoparticles (AuNPs) and investigated the biodistribution of AuNPs in the liver, spleen, kidney, and tumor. The results showed that cisplatin pretreatment increased the levels of ALT and AST in serum, indicating serious toxicity of the liver, which led to more AuNPs accumulation in the damaged liver than in the normal liver. The 5-FU-, IL-2-, IL-6-, or IL-21-treated mice displayed a slight toxicity of the liver, which showed no differences in AuNPs accumulation in the liver between the treated group and the control group. The results also showed that the treatments did not impact the biodistribution of AuNPs in the spleen, kidney, and tumor. These results indicated that cisplatin pretreatment was not suitable for nanomedical cancer therapy, which is essential for the translation and utility of nanotechnology for treating cancer.

Experimental section

General materials

The main materials were 5-fluorouracil (5-FU) (Cat. No. S1209, Selleck Chemicals LLC), cisplatin (Cat. No. 15663-27-1, Merk), IL-2 mouse (Cat. No. HY-P7077, MedChemExpress LLC), IL-6 mouse (Cat. No. HY-P7063, MedChemExpress LLC), IL-21 mouse (Cat. No. HY-P7078, MedChemExpress LLC).

Synthesis of AuNPs

Polyethylene glycol-modified AuNPs were synthesized as previously reported.[6,21] Briefly, 600 μL 1% chloroauric acid ($HAuCl_4$) (R020207-5g, RHWN) was added to 60 mL Milli-Q water and brought to boiling. Next, 240 μL 1% sodium citrate tribasic dihydrate (C8532-500G, Sigma-Aldrich) was added to the

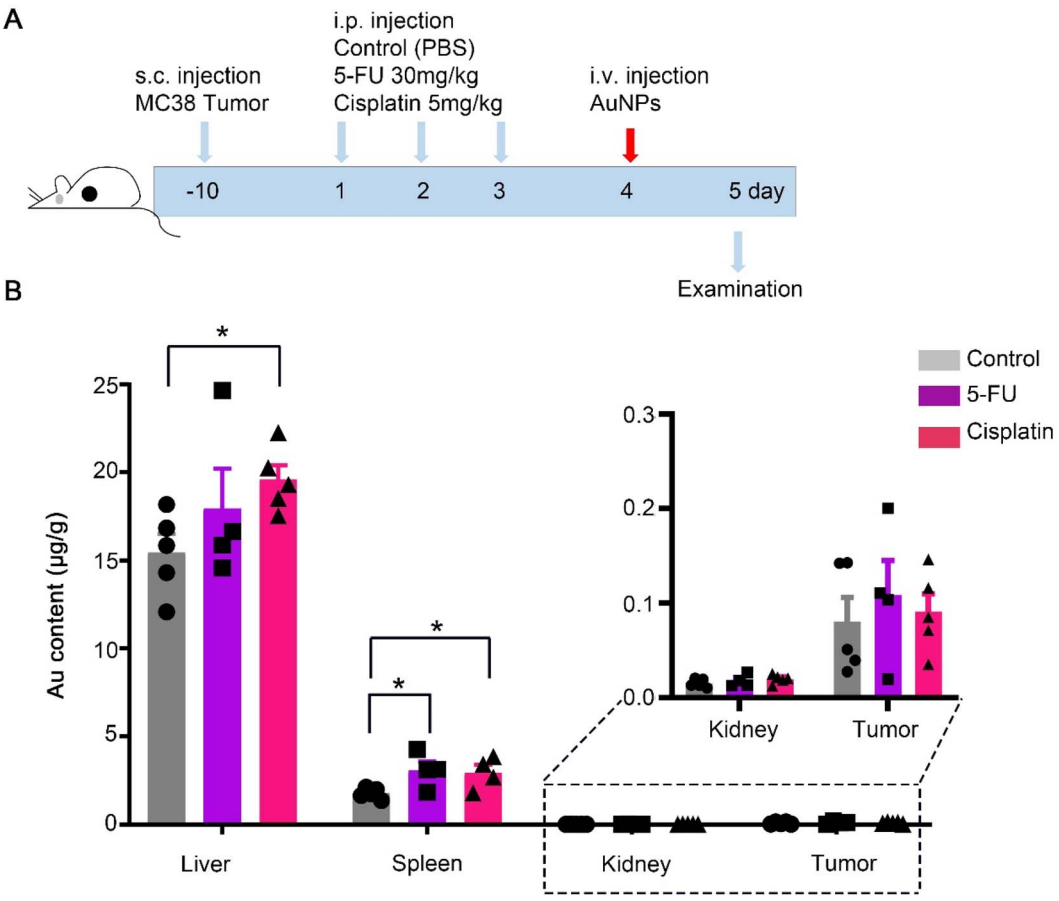

Fig. 1 Biodistribution of AuNPs with control (PBS), 5-FU, and cisplatin treatment. (A) Schematic illustration of the MC38 mouse tumor model with the control, 5-FU, and cisplatin treatment, and AuNPs treatment. (B) Au-content in the liver, spleen, kidney, and tumor by ICP-MS ($n = 4$ or 5). Data presented as the mean ± S. E. M. Statistical analysis was performed by Student's two-tailed t-test. *$p < 0.05$.

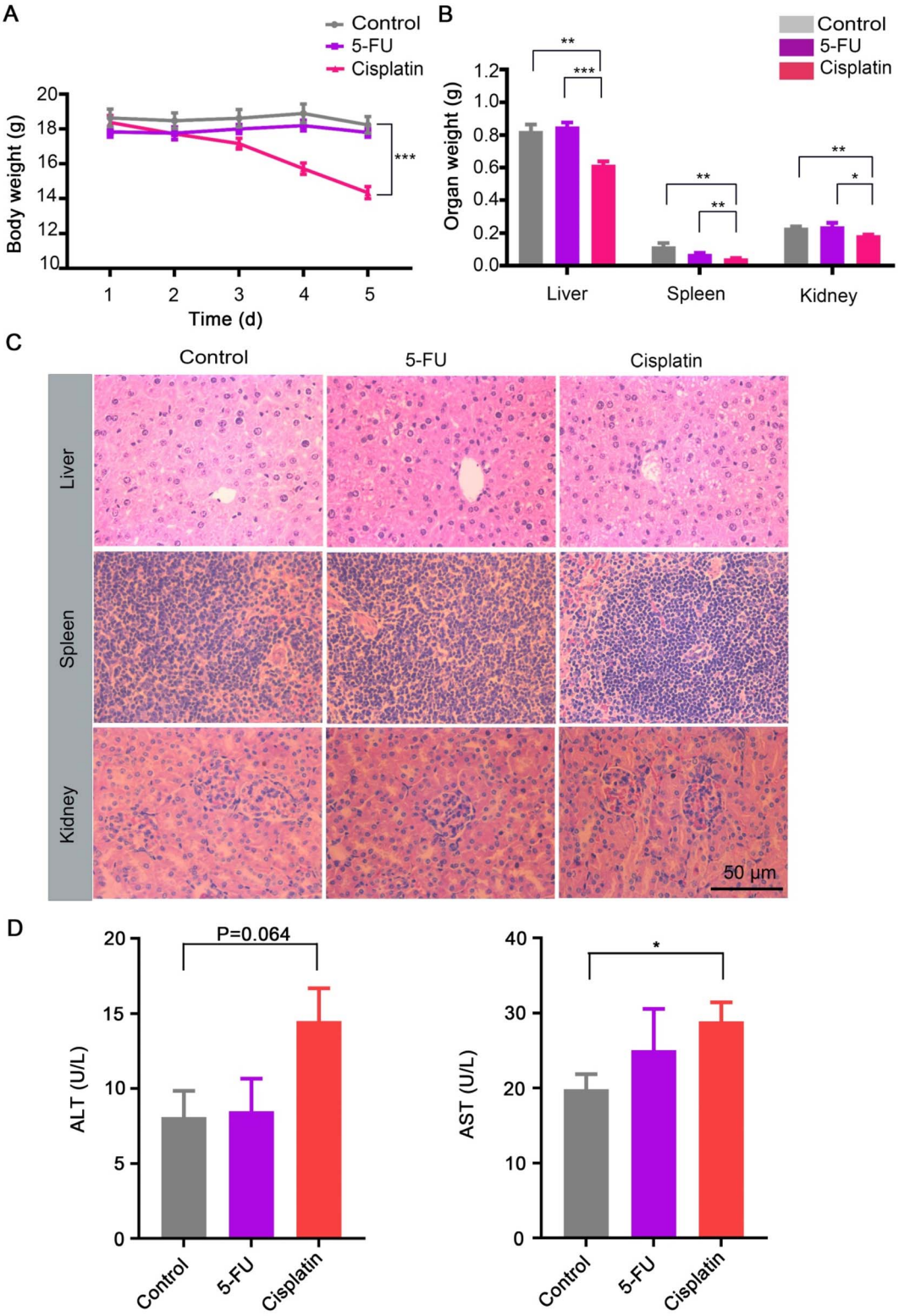

Fig. 2 Physiological index with control (PBS), 5-FU, and cisplatin treatment. (A) Body weight changes of the mice treated with the control, 5-FU, and cisplatin as per Fig. 1A ($n = 5$). Data presented as the mean ± S. E. M. Statistical analysis was performed by Student's two-tailed t-test. ***$p <$ 0.001. (B) Organ weight of the mice treated with the control, 5-FU, and cisplatin ($n = 5$). Data presented as the mean ± S. E. M. Statistical analysis was performed by Student's two-tailed t-test. *$p < 0.05$, **$p < 0.01$, ***$p < 0.001$. (C) Histology of the liver, spleen, and kidney of mice treated with the control, 5-FU, and cisplatin ($n = 5$). (D) Plasma ALT and AST levels after treatment with the control, 5-FU, and cisplatin ($n = 5$). Data presented as the mean ± S. E. M. Statistical analysis was performed by Student's two-tailed t-test. *$p < 0.05$.

solution to synthesize 100 nm AuNPs. The resulting AuNPs were washed with 0.2 mg mL^{-1} sodium citrate tribasic dehydrate twice, and resuspended with Milli-Q water. Then, 5 mg AuNPs were reacted with 5 mg MPEG5000-SH (Ponsure Biotechnology, China) at 60 °C for 1 h. The AuNPs were washed with PBS and stored in PBS at a concentration of 10 mg mL^{-1} and stored at 4 °C.

Animal models

First, 6–8 weeks old C57BL/6 female mice were purchased from Charles River Company and housed in the Laboratory Animal Center of Nantong University (Nantong, China) with a 12 h light–dark cycle and given sterile water and rodent food *ad libitum*. All the animal procedures were performed in accordance with the Guidelines for Care and Use of Laboratory Animals of Nantong University and approved by the Animal Ethics Committee of Institutional Animal Care and Use Committee (IACUC20201201-1001). All the experiments were performed in compliance with all relevant laws or guidelines: regulations on the administration of experimental animals, animal experiment management and technical code, and technical specification for ethical review of laboratory animal welfare in China.

Intraperitoneal injection of the mice with chemotherapy drugs

The MC38 mouse tumor models were obtained by subcutaneous injection with 1×10^6 MC38 cells on the right flank of C57BL/6 mice. The mice (tumor size 0.5 to 0.7 cm in the largest diameter) were divided randomly into three groups: control, 5-FU, and cisplatin ($n = 5$ for each group). First, the control group was intraperitoneally (i.p.) injected with 200 μL PBS every day for three times. The 5-FU group was i.p. injected with 5-FU (30 mg kg^{-1}) every day for three times. The cisplatin group was i.p. injected with cisplatin (5 mg kg^{-1}) every day for three times. After 24 h, all the mice were intravenously (i.v.) injected with 5 mg kg^{-1} AuNPs. After 24 h of AuNPs injection, the mice were sacrificed, and the liver, spleen, kidney, and tumor were collected for further experiments.

Intraperitoneal injection of the mice with interleukins

The MC38 mouse tumor models were obtained as mentioned above. The mice (tumor size 0.5 to 0.7 cm in the largest diameter) were divided randomly into four groups: control, IL-2, IL-6, and IL-21 ($n = 5$ for each group), which were i.p. injected with 200 μL PBS, IL-2 (100 μg kg^{-1}), IL-6 (100 μg kg^{-1}), IL-21 (100 μg kg^{-1}) every day for three times, respectively. After 24 h, all the mice were intravenously (i.v.) injected with 5 mg kg^{-1} AuNPs.

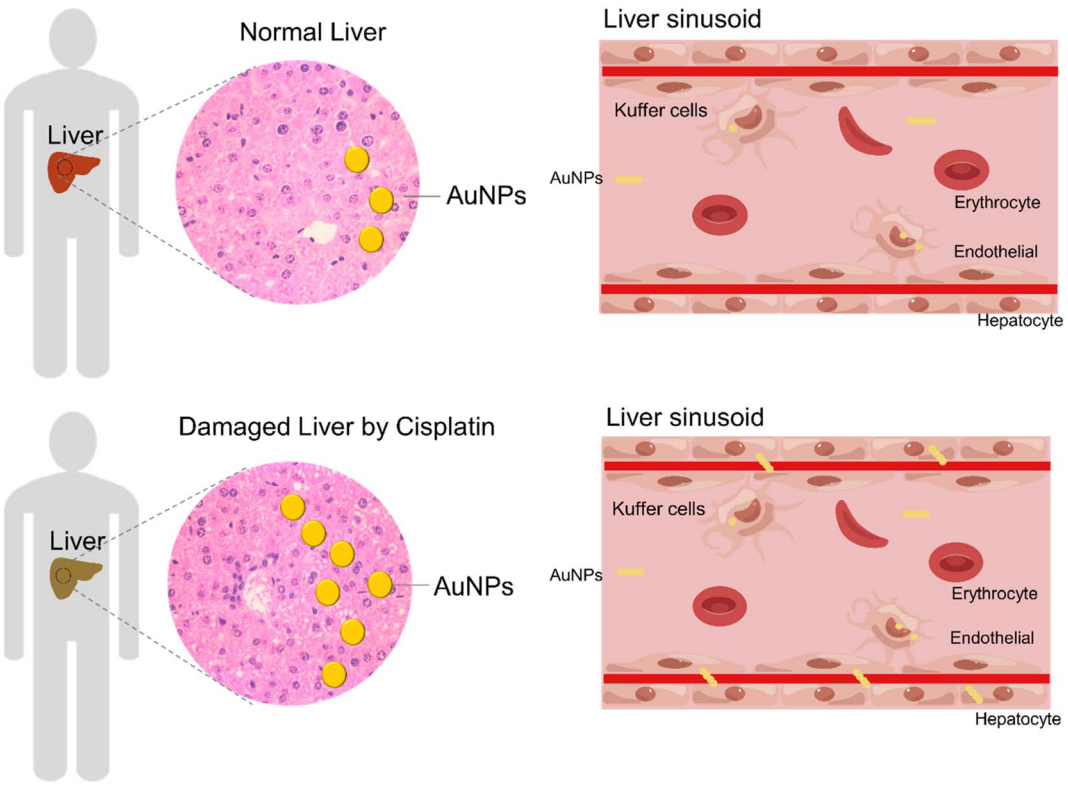

Fig. 3 Comparing AuNPs accumulation in the normal liver or damaged liver by cisplatin treatment. In the normal liver, AuNPs could flow in the liver sinusoid, and be taken up by Kupffer cells and endothelial cells. In the liver damaged by cisplatin treatment, cisplatin induced serious toxicity of the liver. When the AuNPs flowed through the damaged liver, the flow rate of the AuNPs was slower than in the normal liver. The damaged liver would increase the time and space available to accumulate the AuNPs, which increased the AuNPs accumulation in the damaged liver more than in the normal liver.

After 24 h of AuNPs injection, the mice were sacrificed, and the liver, spleen, kidney, and tumor were collected for further experiments.

Au content measured by ICP-MS

For Au analysis, the mice were i.p. injected with chemotherapy drugs. The mice were i.p. injected with interleukins. Then, the liver, spleen, kidney, and tumors of the mice were collected, weighed, and dissolved in aqua regia. The content of Au was measured by inductively coupled plasma-mass spectrometry (ICP-MS; PerkinElmer NexION 350, PerkinElmer, USA).[22]

Histological analysis

The histological stainings of the liver, spleen, and kidney were examined by H & E staining (hematoxylin–eosin staining kit, E607318, Sangon Biotech, China). The histological images were captured under an optical microscope.

Biochemical analysis in serum

Serum aspartate aminotransferase (AST) and alanine aminotransferase (ALT) were analyzed with an analysis kit (Nanjing Jiancheng Bioengineering Institute, China).

Statistical analysis

Student's *t*-test was used for the statistical analysis. The data were presented as the mean ± S. E. M., unless otherwise indicated. $*p < 0.05$, $**p < 0.01$, $***p < 0.001$, $****p < 0.0001$, n. s. indicated no significance.

Results and discussion

To elucidate the effect of chemotherapy on nanomedicine, we mimicked chemotherapy by an acute treatment of 5-FU, or cisplatin, and analyzed the accumulation of AuNPs nanoparticles from a whole organ perspective (Fig. 1A). The MC38 mouse tumor models were pretreated repeatedly with the control, 5-FU, or cisplatin three times, respectively. Then the mice were intravenously injected with 100 nm polyethylene glycol-modified gold nanoparticles (AuNPs) (Fig. S1‡). After 1 d injection of AuNPs, we sacrificed the mice and quantified gold biodistribution in the tissues by ICP-MS. We found that the accumulations of AuNPs in the liver and spleen increased significantly after cisplatin treatment compared with the control, and the accumulation of AuNPs in the spleen increased significantly after the 5-FU treatment compared with the control (Fig. 1B). There were no differences in the accumulations in the

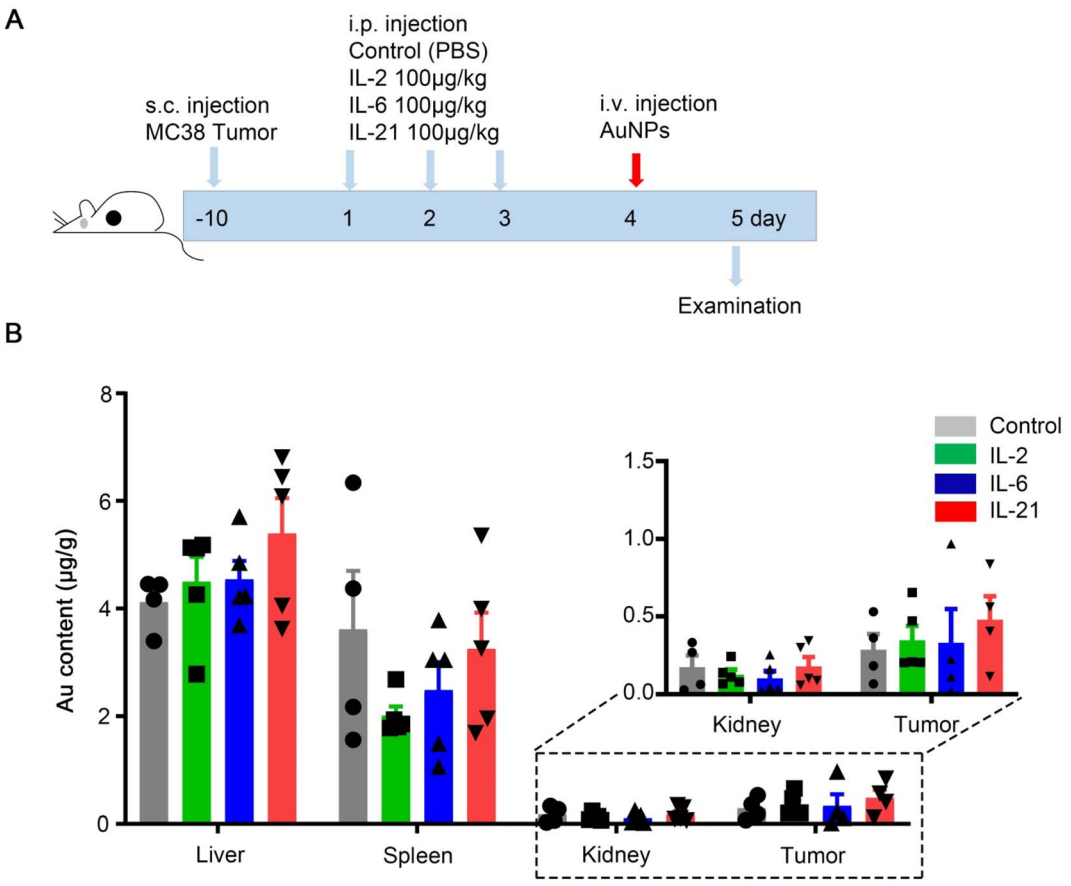

Fig. 4 Biodistribution of AuNPs with control (PBS), IL-2, IL-6, and IL-21 treatment. (A) Schematic illustration of the MC38 mouse tumor model with the control, IL-2, IL-6, and IL-21 treatment, and AuNPs treatment. (B) Au-content in the liver, spleen, kidney, and tumor by ICP-MS ($n = 4$ or 5). Data presented as the mean ± S. E. M.

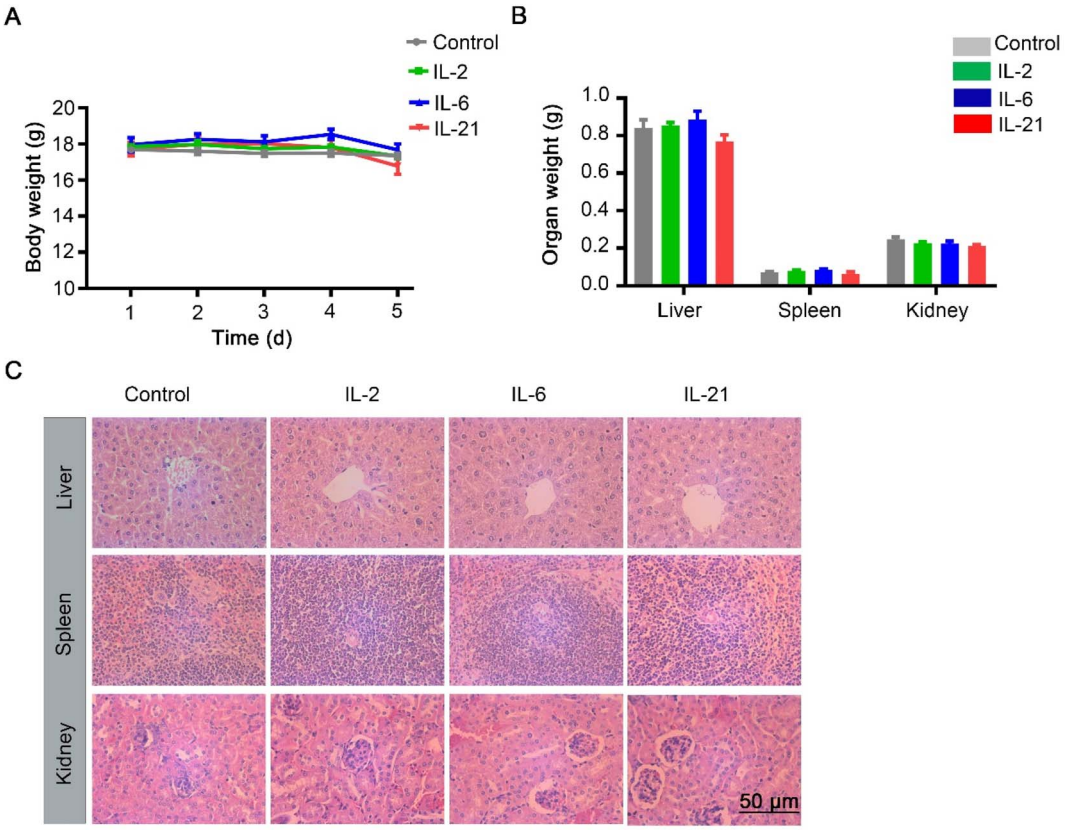

Fig. 5 Physiological index with control (PBS), IL-2, IL-6, and IL-21 treatment. (A) Body weight changes of the mice treated with the control, IL-2, IL-6, and IL-21 as per Fig. 3A ($n = 5$). Data presented as the mean ± S. E. M. (B) Organ weight of mice treated with the control, IL-2, IL-6, and IL-21 ($n = 5$). Data presented as the mean ± S. E. M. (C) Histology of the liver, spleen, and kidney of the mice treated with control, IL-2, IL-6, and IL-21 ($n = 5$).

kidney and tumor among the control, 5-FU, and cisplatin treatment groups (Fig. 1B). The results indicated that 5-FU and cisplatin did not affect the AuNPs entering tumors. However, cisplatin increased the AuNPs entering the liver and spleen, which indicated that AuNPs accumulated more in the damaged liver than normal liver.

Next, we investigated the reason of the AuNPs retained more in the liver after cisplatin treatment than after PBS treatment. The liver is the largest reticuloendothelial system (RES) organ and took up most of the administered nanoparticles.[22,23] When the nanoparticles entered the liver, the flow rate of the nanoparticles slowed 1000 times in the liver sinusoid, and most of the nanoparticles were taken up by hepatic Kupffer cells, B cells, and endothelial cells. We hypothesized that the cisplatin-induced hepatotoxicity reduced the liver clearance of AuNPs. Therefore, we investigated the toxicity of cisplatin and 5-FU treatment. The treatment procedure was as the same as shown in Fig. 1A. The results showed that the body weight decreased significantly with cisplatin treatment compared with the control and the 5-FU treatment (Fig. 2A). The weights of the liver, spleen, and kidney decreased significantly with cisplatin treatment compared with the control and 5-FU treatment, and 5-FU just caused a slight toxicity (Fig. 2B). We also found that cisplatin-induced observed hepatocyte necrosis (Fig. 2C). Finally, the serum ALT and AST levels were elevated. The results showed that cisplatin treatment significantly increased the levels of ALT and AST in serum (Fig. 2D).[24,25] The results showed that cisplatin induced more serious toxicity of the liver than the 5-FU and the control groups. 5-FU just caused slightly more toxicity than the control group. There are reasons to believe that when the AuNPs flow through the damaged liver, the flow rate of the AuNPs would be slower than in the normal liver. The damaged liver would increase the time and space available to accumulate the AuNPs. We predicted that the cisplatin-induced hepatotoxicity reduced the liver clearance of AuNPs, which increased the AuNPs accumulation in the damaged liver more than in the normal liver (Fig. 3).

To elucidate the effect of immunotherapy on nanomedicine, we used immunotherapy by IL-2, IL-6, or IL-21 treatment, and analyzed the accumulation in the organs. A schematic illustration of the MC38 mouse tumor models treated repeatedly with the control, IL-2, IL-6, or IL-21 three times is shown in Fig. 4A. Then, the mice were intravenously injected with 100 nm polyethylene glycol-modified AuNPs (Fig. 4A). After 1 d injection of AuNPs, we sacrificed the mice and quantified the gold biodistribution in the tissues by inductively coupled plasma-mass spectrometry (ICP-MS). We found that the accumulations of AuNPs in the liver, spleen,

kidney, and tumor were not significantly different among all the groups (Fig. 4B). The results indicated that IL-2, IL-6, and IL-21 did not affect the AuNPs entering tumors. We also investigated the toxicity of these chemokines. The results showed that the body weight and organ weights were not significantly different in IL-2, IL-6, or IL-21 treatment compared with the control (Fig. 5A and B). The histology staining showed that IL-2, IL-6, or IL-21 treatment did not cause significant toxicity to the liver, spleen, or kidney (Fig. 5C). These results indicated that IL-2, IL-6, or IL-21 treatment did not affect the accumulation of AuNPs in the body.

Conclusions

Comparing the biodistribution of AuNPs in the liver, spleen, kidney, and tumor among the control, chemotherapy, and immunotherapy, it could be predicted whether the nanomedicine used or not after the priority treatment strategy failed. We focused on the questions (I) is there a difference in nanoparticles uptake between the normal liver and damaged liver? The results showed that when the AuNPs flowed through the liver damaged by cisplatin treatment, the flow rate of the AuNPs was slower than in the normal liver. The damaged liver would increase the time and space available to accumulate the AuNPs. We predicted that the cisplatin-induced hepatotoxicity reduced the liver clearance of AuNPs, which increased the AuNPs accumulation in this damaged liver more than in the normal liver; (II) does the damaged liver impact nanoparticles entering the solid tumor? The data showed that the accumulation of AuNPs in the liver damaged by cisplatin treatment was increased compared to in the normal liver. However, the accumulation of AuNPs in the tumor showed no changes. These results indicated that cisplatin pretreatment was not suitable for subsequent nanomedical cancer therapy. These findings suggest that low-toxicity treatment may be the better priority treatment strategy before nanomedical cancer therapy.

Author contributions

Conceptualization and supervision: G. Wang and W. Li. Investigation, methodology and validation: P. Wu., Y. Zhang and S. Zhu. methodology, validation: M. Wang and P. Zhou. Writing – original draft and writing – review & editing: P. Wu., Y. Zhang., S. Zhu., G. Wang and W.·Li.

Conflicts of interest

The authors declare no competing financial interest.

Acknowledgements

This work was supported by Jiangsu Specially-Appointed Professor (06200054 to W. L.), and Startup fund from Nantong University (W. L.). We thank the figdraw platform with the image design of liver sinusoid (Approved ID: ITSIW08827).

References

1 M. J. Mitchell, M. M. Billingsley, R. M. Haley, M. E. Wechsler, N. A. Peppas and R. Langer, *Nat. Rev. Drug Discovery*, 2021, **20**, 101–124.
2 S. Rawal and M. M. Patel, *J. Control Release*, 2019, **301**, 76–109.
3 Y. Wang, Z. Zhang, C. Zheng, X. Zhao, Y. Zheng, Q. Liu, Y. Liu and L. Shi, *Small*, 2021, **17**, e2100578.
4 P. Zhang, Y. Zhang, X. Ding, W. Shen, M. Li, E. Wagner, C. Xiao and X. Chen, *Adv. Mater.*, 2020, **32**, e2000013.
5 B. Ouyang, W. Poon, Y.-N. Zhang, Z. P. Lin, B. R. Kingston, A. J. Tavares, Y. Zhang, J. Chen, M. S. Valic, A. M. Syed, P. MacMillan, J. Couture-Senécal, G. Zheng and W. C. W. Chan, *Nat. Mater.*, 2020, **19**, 1362–1371.
6 A. J. Tavares, W. Poon, Y.-N. Zhang, Q. Dai, R. Besla, D. Ding, B. Ouyang, A. Li, J. Chen, G. Zheng, C. Robbins and W. C. W. Chan, *Proc. Natl. Acad. Sci. U. S. A.*, 2017, **114**, E10871–E10880.
7 K. M. Tsoi, S. A. MacParland, X.-Z. Ma, V. N. Spetzler, J. Echeverri, B. Ouyang, S. M. Fadel, E. A. Sykes, N. Goldaracena, J. M. Kaths, J. B. Conneely, B. A. Alman, M. Selzner, M. A. Ostrowski, O. A. Adeyi, A. Zilman, I. D. McGilvray and W. C. W. Chan, *Nat. Mater.*, 2016, **15**, 1212–1221.
8 T. Tanvetyanon, *N. Engl. J. Med.*, 2022, **387**, 571.
9 K. Shitara, J. A. Ajani, M. Moehler, M. Garrido, C. Gallardo, L. Shen, K. Yamaguchi, L. Wyrwicz, T. Skoczylas, A. C. Bragagnoli, T. Liu, M. Tehfe, E. Elimova, R. Bruges, T. Zander, S. de Azevedo, R. Kowalyszyn, R. Pazo-Cid, M. Schenker, J. M. Cleary, P. Yanez, K. Feeney, M. V. Karamouzis, V. Poulart, M. Lei, H. Xiao, K. Kondo, M. Li and Y. Y. Janjigian, *Nature*, 2022, **603**, 942–948.
10 Y. Y. Janjigian, K. Shitara, M. Moehler, M. Garrido, P. Salman, L. Shen, L. Wyrwicz, K. Yamaguchi, T. Skoczylas, A. Campos Bragagnoli, T. Liu, M. Schenker, P. Yanez, M. Tehfe, R. Kowalyszyn, M. V. Karamouzis, R. Bruges, T. Zander, R. Pazo-Cid, E. Hitre, K. Feeney, J. M. Cleary, V. Poulart, D. Cullen, M. Lei, H. Xiao, K. Kondo, M. Li and J. A. Ajani, *Lancet*, 2021, **398**, 27–40.
11 S. Ghosh, *Bioorg. Chem.*, 2019, **88**, 102925.
12 W. Ben Ayed, A. Ben Said, A. Hamdi, A. Mokrani, Y. Masmoudi, I. Toukabri, I. Limayem and Y. Yahyaoui, *J. Oncol. Pharm. Pract.*, 2020, **26**, 1621–1629.
13 D. B. Longley, D. P. Harkin and P. G. Johnston, *Nat. Rev. Cancer*, 2003, **3**, 330–338.
14 S. Hussain, *Trends Cancer*, 2020, **6**, 365–368.
15 F. Alessandrino, L. Qin, G. Cruz, S. Sahu, M. H. Rosenthal, J. A. Meyerhardt and A. B. Shinagare, *Abdom. Radiol.*, 2019, **44**, 3099–3106.
16 D. J. Propper and F. R. Balkwill, *Nat. Rev. Clin. Oncol.*, 2022, **19**, 237–253.
17 S. A. Atallah-Yunes and M. J. Robertson, *Front. Immunol.*, 2022, **13**, 872010.
18 Y. Hailemichael, D. H. Johnson, N. Abdel-Wahab, W. C. Foo, S.-E. Bentebibel, M. Daher, C. Haymaker, K. Wani,

C. Saberian, D. Ogata, S. T. Kim, R. Nurieva, A. J. Lazar, H. Abu-Sbeih, F. Fa'ak, A. Mathew, Y. Wang, A. Falohun, V. Trinh, C. Zobniw, C. Spillson, J. K. Burks, M. Awiwi, K. Elsayes, L. S. Soto, B. D. Melendez, M. A. Davies, J. Wargo, J. Curry, C. Yee, G. Lizee, S. Singh, P. Sharma, J. P. Allison, P. Hwu, S. Ekmekcioglu and A. Diab, *Cancer Cell*, 2022, **40**, 509–523.

19 W. W. Overwijk, M. A. Tagliaferri and J. Zalevsky, *Annu. Rev. Med.*, 2021, **72**, 281–311.

20 S. Deng, Z. Sun, J. Qiao, Y. Liang, L. Liu, C. Dong, A. Shen, Y. Wang, H. Tang, Y.-X. Fu and H. Peng, *JCI Insight*, 2020, **5**, e132000.

21 S. D. Perrault and W. C. W. Chan, *J. Am. Chem. Soc.*, 2009, **131**, 17042–17043.

22 Y. Huang, S. Zhu, P. Wu, S. Gong, W. Li and F. Sun, *ACS. Appl. Nano Mater.*, 2021, **4**, 13919–13926.

23 Y.-N. Zhang, W. Poon, A. J. Tavares, I. D. McGilvray and W. C. W. Chan, *J. Control Release*, 2016, **240**, 332–348.

24 S. Wilhelm, A. J. Tavares, Q. Dai, S. Ohta, J. Audet, H. F. Dvorak and W. C. W. Chan, *Nat. Rev. Mater.*, 2016, **1**, 1–12.

25 X. Qu, H. Gao, L. Tao, Y. Zhang, J. Zhai, J. Sun, Y. Song and S. Zhang, *J. Toxicol. Sci.*, 2019, **44**, 167–175.